The Canadian Mineralogist
Vol. 33, pp. 435-444 (1995)

A CRITICAL LOOK AT QUANTITATIVE LASER-ABLATION ICP–MS ANALYSIS OF NATURAL AND SYNTHETIC GLASSES

JOHN STIX, GILLES GAUTHIER AND JOHN N. LUDDEN

Département de géologie, Université de Montréal, Case postale 6128, succursale Centre-ville, Montréal, Québec H3C 3J7

ABSTRACT

In this paper, we examine techniques and problems of quantitative laser-ablation ICP–MS analysis for natural and synthetic glass samples and discuss internal standardization, use of calibration curves, and single-standard calibration. Internal standards are used to normalize raw intensities and are generally a low-abundance isotope of a major element in the samples. For zoned minerals, internal standards are used that show small compositional variations. Calibration curves are necessary to define the ICP–MS response over a range of concentrations and are constructed using a series of geochemical reference standards of similar composition to the unknown materials to be analyzed. A series of calibration curves for mafic–ultramafic and felsic glasses are presented, which generally show linear behavior. However, Zr, Y, and Ce calibrations are nonlinear and exhibit higher relative intensities for these elements at higher concentrations. This nonlinearity may be the result of (1) large ranges in concentrations or (2) matrix effects involving iron and total trace-element content in the glasses. Calibrations using a single geochemical reference standard can be attempted only if the calibration curves are linear and pass through the origin, and if the reference standard and the samples have similar compositions.

Keywords: laser-ablation ICP–MS, inductively coupled plasma – mass spectrometry, trace elements, glass, calibration.

SOMMAIRE

Cet article examine certaines techniques quantitatives d'ablation au laser en analyse par ICP–MS de verres naturels et synthétiques. Nous discutons de l'utilisation des étalons internes, des courbes de calibrage et de calibrage avec un seul échantillon géochimique de référence. Les étalons internes sont utilisés pour faire la normalisation des intensités brutes d'un isotope d'un élément trace; ces étalons sont généralement un isotope de faible abondance d'un élément majeur dans les échantillons. Pour les minéraux zonés, on utilise des étalons internes montrant de faibles variations compositionnelles. Des courbes de calibrage sont nécessaires afin de définir la réponse de l'ICP–MS pour une gamme de concentrations; ces courbes comprennent une série d'échantillons géochimiques de référence dont la composition est semblable à celle de l'échantillon inconnu. Nous présentons une série de courbes de calibrage pour des verres ultramafiques–mafiques et felsiques. Ces courbes montrent généralement un comportement linéaire. Cependant, les courbes de calibrage pour le Zr, le Y et le Ce ne sont pas linéaires et montrent des intensités anormalement élevées à haute concentration. Ces resultats peuvent être causés par (1) une grande gamme de concentrations ou (2) un effet de matrice qui implique le fer et le contenu total des éléments traces dans l'échantillon. Des calibrages qui utilisent un seul échantillon géochimique de référence sont valables seulement si les calibrages sont linéaires, recoupant l'origine. De plus, l'étalon et l'échantillon inconnu doivent avoir des compositions semblables.

Mots-clés: ablation laser par ICP–MS, plasma à couplage inductif avec spectrométrie de masse, éléments traces, verre, calibrage.

INTRODUCTION

Trace-element analysis by laser-ablation inductively coupled plasma – mass spectrometry (ICP–MS) is a rapidly developing technique. The burgeoning literature regarding this method attests to its capability to analyze small volumes of material at the sub-ppm level. Early use of laser-ablation systems were designed to circumvent the problems of putting rocks and minerals into solution. Hence, the systems were designed for bulk sampling of solid materials, and laser-spot sizes were typically larger than 100 µm. In recent years, laser-ablation systems have been modified by frequency doubling and quadrupling to utilize their micro-analytical potential. Currently, spot sizes using infrared (1064 nm) and ultraviolet (266 nm) Nd:YAG laser-ablation systems are on the order of 10–60 µm depending on the solid analyzed, the laser's energy and its wavelength. We expect that the size of the focused laser beam will decrease to less than 10 µm in the next few years.

Laser-ablation ICP–MS is a comparatively new technique, and calibration procedures for geological materials have not yet been systematically studied. Some researchers prefer to match matrices of standards and samples, and use a series of standard calibration curves (Pearce *et al.* 1992, Perkins *et al.* 1992, 1993), whereas others use a single standard to determine trace element contents in the samples (Jackson *et al.* 1992, Jenner *et al.* 1993). A combination of these techniques also has been used (Fedorowich *et al.* 1993, Jarvis & Williams 1993). It appears that some of these techniques work better than others, particularly where the goal is quantitative analysis at better than 5% accuracy. The important question of how laser-ablation ICP–MS responds to materials of different matrices (*e.g.*, olivine *versus* pyroxene) has not been studied in a systematic fashion. It is our purpose in this paper to examine calibration procedures used in laser-ablation ICP–MS analysis and to propose a methodology for quantitative calibration of geologically important trace elements at the ppm and ppb levels in glass samples.

TABLE 1. CHOICES OF INTERNAL STANDARDS IN GLASSES AND MINERALS

Material	Internal standard*
mafic glasses	^{44}Ca, ^{57}Fe, ^{29}Si
felsic glasses	^{29}Si (^{57}Fe)
plagioclase	^{29}Si, ^{44}Ca
alkali feldspar	^{29}Si (^{44}Ca)
amphibole	^{44}Ca, ^{29}Si (^{57}Fe, ^{25}Mg)
olivine	^{29}Si (^{57}Fe, ^{25}Mg)
titaniferous magnetite	^{57}Fe, ^{49}Ti
ilmenite	^{49}Ti, ^{57}Fe
orthopyroxene	^{29}Si (^{57}Fe, ^{25}Mg)
clinopyroxene	^{29}Si (^{57}Fe, ^{44}Ca, ^{25}Mg)
garnet	^{29}Si (^{57}Fe, ^{44}Ca, ^{25}Mg)
biotite	^{29}Si, ^{49}Ti (^{57}Fe, ^{25}Mg)

* Isotopes are arranged in order of decreasing preference as internal standards. Isotopes shown in parentheses are less strongly recommended owing to their potential for being zoned in the mineral.

INTERNAL STANDARDIZATION

Because different amounts of material are ablated by the laser from one spot to the next in a fixed time-interval, it is difficult to use absolute intensities of signals for calibration purposes. Instead, the intensity is normalized relative to the intensity of another isotope, *i.e.*, the internal standard, the concentration of which is known. This ratio is then multiplied by the concentration of the internal standard, giving a normalized ratio of intensity. The internal standard is generally a major element whose concentration has been previously determined by electron microprobe (EMP), X-ray fluorescence (XRF) or solution ICP–MS. In this study, characterization of the glasses was accomplished by these bulk techniques before beginning laser work. Ideally, a good rule to follow in selecting an internal standard is to use the lowest-abundance isotope of the most abundant element in the material to be analyzed. For silicates, one would thus use ^{30}Si, which has a relative abundance of 3.09%. However, nitrogen oxide produces a high background at mass 30, such that it is preferable to use ^{29}Si, with an abundance of 4.7%. In practice, other major elements (*e.g.*, Ca, Fe) may serve as well or better than Si, depending on the type of glass or mineral, presence or absence of zoning, and the geochemical similarity between standard and sample (Table 1). When analyzing an unknown mineral initially, it is good practice to use two or more internal standards to check consistency, precision and accuracy.

Minerals that are zoned pose a problem because the electron microprobe analyzes a much smaller volume than does the laser. If the concentration of an internal standard changes as a function of depth, therefore, an error will result when calculating the normalized ratio because the internal standard's concentration has been assumed to be constant. There are two solutions to this problem. First, if the sample surface is unzoned, the laser can be rastered to minimize depth sampling. Second, one can choose an internal standard whose concentration varies little in zoned minerals. For example, the concentration of silica in an alkali feldspar changes only about 3 wt.% despite large changes in Na and K contents. Similarly, Ca in igneous amphiboles varies less than Si, Mg, and Fe.

USE OF CALIBRATION CURVES

Quantitative laser-ablation ICP–MS analysis can be accomplished using a series of well-characterized geochemical reference standards whose major-element compositions are similar to those of the unknown materials to be analyzed. The resulting calibration curves are ideally linear and intersect the origin. Calibration curves are useful to define the instrument's

TABLE 2. TYPICAL OPERATING CONDITIONS OF THE ICP-MS AND LASER

Parameter	Value
Expansion vacuum	2.4 mbar
Intermediate vacuum	10^{-4} mbar
Analyzer vacuum	1.3×10^{-6} mbar
Plasma gas flow	13.5 L/min
Auxiliary gas flow	0.8 L/min
Carrier gas flow	1.19 L/min
Incident power	1350 kW
Reflected power	1 W
Peak shape; full mass-resolution	4.8 V
high mass-resolution	2.6 V
Extraction lens	-135 V
Collector lens	3 V
L1 lens	1 V
L2 lens	-30 V
L3 lens	11 V
L4 lens	-50 V
Front Plate lens	0 V
Pole bias lens	-2 V
Laser mode	Q-switched
Laser flashlamp voltage	945 V
Laser energy	3.6 mjoule/shot
Laser repetition rate	4 Hz
Data acquisition mode	peak jumping
Points per peak	3
DAC steps	1
Dwell time per point	10.24 ms

response over a range of concentrations, and they should be applied before using single standards to calibrate.

For this study, our methodology permitted us to analyze samples rapidly and precisely with the laser in Q-switched mode. When analyzing standards, we generally did three to four replicate analyses using three consecutive periods of acquisition for an individual analysis. The precision of replicate determinations on individual homogeneous glasses was better than 10% relative, except for elements of low concentration (<1 ppm), for which precision is 10% or worse. Background interference was subtracted by running a gas blank before analyzing the glasses. For our instrument, the limit of detection for most elements is about 1 ppm. Typical operating conditions for the ICP–MS and the laser are given in Table 2. In the following sections, a series of calibrations for ultramafic–mafic and rhyolitic glasses are presented using a series of natural and synthetic glasses for calibration. These standards have been previously characterized for major and trace elements by a variety of techniques (see Tables 3, 4; Appendix 1), they are aphyric and homogeneous on the scale of the size of the laser crater, and there is abundant material available both as chips and powders. Note that Appendix 1 is available from the Depository of Unpublished Data, CISTI, National Research Council of Canada, Ottawa, Ontario K1A 0S2.

TABLE 3. WORKING VALUES FOR ULTRAMAFIC AND MAFIC STANDARD GLASSES

Element	P1326-2	P-MT	73	HF-13
SiO_2 wt.%	50.00	40.43	51.66	41.44
TiO_2	1.53	3.81	1.73	2.46
Al_2O_3	14.48	14.47	16.61	11.58
FeO*	10.82	8.77	7.70	12.23
MnO	0.16	0.09	0.16	0.23
MgO	7.30	14.48	4.47	11.36
CaO	12.18	12.34	8.65	11.02
Na_2O	2.76	1.92	4.77	5.12
K_2O	0.17	2.29	2.00	2.01
P_2O_5	0.12	0.04	0.53	1.46
Total	99.52	98.64	98.12	98.91
Li ppm	5.2	2.7	8.9	12
Be	0.3		2.6	
B	0.5		3.7	
Rb	2.15	17	41	29
Cs	0.021	0.02		0.2
Sr	153	469	576	1516
Ba	38	363	340	326
Pb	1.1	4.2		0.56
Co	47		34	
Ni	46		76	
Cu	94			
Zn	87			
Cr	313		85	
Sc	47			
La	4.7	5.8	46	83
Ce	12.7	18	98	162
Pr	2.1	3.0		20
Nd	10.8	15	41	74
Sm	3.4	3.8	7.9	14
Eu	1.3	1.3	2.3	4.5
Gd	4.6	4.1		11
Tb	0.76	0.50	1.0	1.5
Dy	5.3	2.6		7.0
Ho	1.1	0.44		1.1
Y	33	11	30	28
Er	3.3	1.1		2.6
Tm	0.50	0.13		0.29
Yb	3.1	0.71	2.9	1.5
Lu	0.44	0.093	0.40	0.19
Hf	2.6	2.3		6.2
Zr	94	53	323	299
Th	0.36	0.20		9.2
V			201	
Nb	4.4	15	63	107
Ta	0.28	1.0		5.8
U	0.13	0.055		2.8

Sources of data: P1326-2 analyzed for major elements by electron microprobe at McGill University and for trace elements by XRF, INAA, and solution ICP-MS at the Université de Montréal and by solution ICP-MS at Memorial University; P-MT analyzed by C. Dalpé for major elements by electron microprobe at McGill University and for trace elements by solution ICP-MS at the Université de Montréal and Memorial University (Dalpé et al. 1995); 73 analyzed by B. Cousens for major elements by electron microprobe at the University of British Columbia (Allan et al. 1993) and for trace elements (whole-rock) by XRF at the University of British Columbia and by INAA at the University of Rhode Island (Cousens et al. 1985); HF-13 analyzed by C. Dalpé for major elements by electron microprobe at McGill University and for trace elements by solution ICP-MS at the Université de Montréal and Memorial University (Dalpé et al. 1995). Full compilation of data for P1326-2 is found in Appendix 1. * Total iron expressed as FeO.

Calibration of mafic and ultramafic glasses

We used four glass standards to calibrate mafic and ultramafic glasses: P1326–2 (Juan de Fuca MORB), P–MT (glass of pargasite composition), HF–13 (nephelinitic glass) and 73 (alkaline basalt glass) (Table 3, Appendix 1). Standard P1326–2 and 73 are natural glasses, whereas P–MT and HF–13 are synthetic glasses fused from mineral and rock powders by repeated melting at 1400°C and 1 atmosphere under controlled oxygen fugacity (Dalpé *et al.* 1995). Standard P1326–2, HF–13, and P–MT have been characterized thoroughly by ICP–MS solution analysis, X-ray fluorescence (XRF), instrumental neutron-activation analysis (INAA), and other techniques. Standard 73 is less well characterized than the other glasses.

Figure 1 shows typical calibration curves for Ce and Zr by laser-ablation ICP–MS analysis. For Ce, the calibrations using three internal standards (^{29}Si, ^{44}Ca, ^{57}Fe) are generally linear over 150 ppm Ce (Fig. 1a). The Ca-normalized calibration is more variable, possibly as a result of some uncertainty in the accepted values of Ca or Ce for standard 73. In contrast with Ce, Zr exhibits variable behavior depending on the internal standard that is used to normalize the intensities. We have plotted the Zr data using ^{29}Si, ^{44}Ca, and ^{88}Sr as internal standards with two different pre-ablation times (30 and 90 seconds) (Figs. 1b–d). Using our best-characterized glasses (P1326–2, P–MT, and HF–13), with a range of about 250 ppm Zr, the Si- and Ca-normalized calibrations are nonlinear, whereas the Sr-normalized calibration is linear. In detail, the Si- and Ca-normalized Zr intensities for HF–13 are anomalously high compared to those for P1326–2 and P–MT. As a result, the Si- and Ca-normalized calibration curves

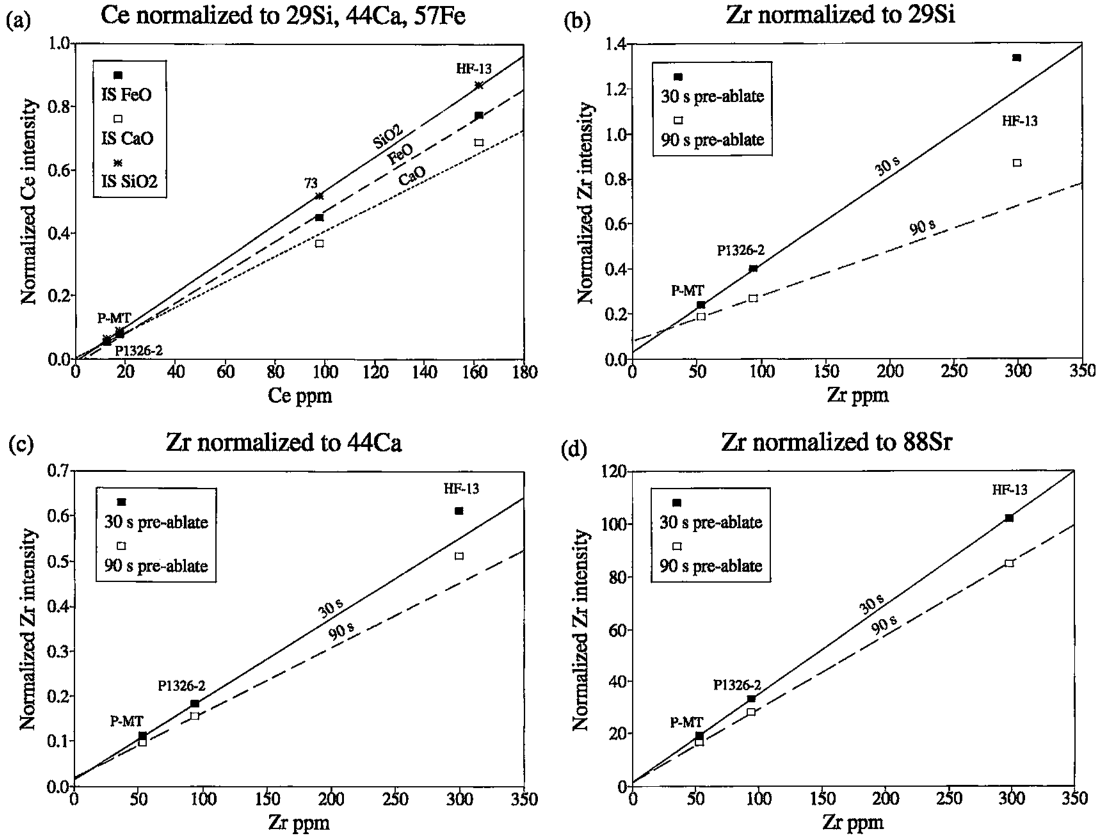

FIG. 1. Calibration curves for mafic and ultramafic glasses. Concentrations are plotted against the normalized intensity of a trace element, which is the element's intensity measured by ICP–MS divided by that of the internal standard, multiplied by the internal standard's concentration. (a) ^{140}Ce calibration using ^{29}Si, ^{44}Ca, and ^{57}Fe as internal standards (b) ^{90}Zr calibration using ^{29}Si as internal standard and pre-ablation times of 30 and 90 seconds (c) ^{90}Zr calibration using ^{44}Ca as internal standard and pre-ablation times of 30 and 90 seconds, and (d) ^{90}Zr calibration using ^{88}Sr as internal standard and pre-ablation times of 30 and 90 seconds.

seem to become steeper at high concentrations of Zr. This lack of linearity is observed for both pre-ablation times, suggesting that this parameter does not influence the relative intensities of the different samples. The reproducibility of the results for two different internal standards (Si, Ca) and for different pre-ablation times strongly suggests that the effect is real. In contrast, the Sr-normalized calibration, for both 30 s and 90 s pre-ablation, is linear. It appears that the Zr intensity increases with respect to that of Si and Ca, but not that of Sr, as the Zr concentration increases. This fractionation effect may be caused by the relatively large differences in mass between Zr on the one hand and Si and Ca on the other. In comparison, Zr and Sr have a similar mass and probably more similar behavior during laser ablation, thus minimizing fractionation between the two elements. The Zr calibrations also differ from those for other trace elements such as Sm and Eu by covering a much larger range of concentration (*e.g.*, 250 ppm Zr *versus* 10 ppm Sm, and 4 ppm Eu; see Table 3). These data suggest that Zr in mafic and ultramafic glasses may be difficult to calibrate accurately using these major elements as internal standards if the samples have a wide range of Zr contents. If the samples have less than 100 ppm Zr, the data for P1326–2 and P–MT, which indicate a linear relationship intersecting close to the origin, can be used for calibration.

Calibration of felsic glasses

For the calibration of felsic glasses, we use various combinations of seven glasses: two synthetic glasses (NIST–612/613 and NIST–610/611), two natural metaluminous obsidian glasses (UDM–1 and DM–0), and three natural peralkaline obsidian glasses (UTR–2, KN–9 and KE–12) (Table 4, Appendix 1). NIST–612/613, UDM–1, and UTR–2 are well-characterized glasses, whereas NIST–610/611, DM–0, KN–9, and KE–12 are not as thoroughly characterized. Compared to the natural obsidian glasses, the synthetic glasses have low concentrations of Al, K and Fe, and high concentrations of Na and Ca. The five obsidian samples have rather similar major-element compositions, except that concentrations of Fe and Na are higher, and those of Si and Al are lower, in the peralkaline glasses. For routine analytical work, NIST–612/613, UDM–1 and UTR–2 are used for calibration and generally give linear responses.

TABLE 4. WORKING VALUES FOR FELSIC STANDARD GLASSES

Element	NIST–612	NIST–610	UDM–1	DM–0	UTR–2	KN–9	KE–12
SiO_2 wt.%	71.5	70.70	76.81	76.57	74.16	74.7	70.3
TiO_2		0.07	0.14	0.09	0.24	0.18	0.33
Al_2O_3	2.15	2.00	12.83	12.29	10.44	10.47	7.62
Fe_2O_3*	0.03	0.06	0.91	1.12	4.43	3.86	9.29
MnO		0.05	0.06	0.06	0.09	0.06	0.26
MgO	0.02	0.06	0.11	0.19	0.05	0.01	0.02
CaO	11.4	12.09	0.84	0.35	0.18	0.14	0.35
Na_2O	13.0	14.35	4.13	4.29	5.52	5.48	7.28
K_2O	0.02	0.06	4.23	4.65	4.39	4.44	4.27
P_2O_5				0.01	0.01		0.02
H_2O^+				0.39			
H_2O^-				0.07	0.32		
F		0.04	0.05		0.13	0.64	0.44
Cl		0.04	0.01		0.21	0.31	0.33
O≡F,Cl		0.03	0.02		0.10	0.34	0.26
Total	98.12	99.49	100.10	100.08	100.07	99.95	100.26
Li ppm	39.1	456	35		61		
Be	38.7	410			9.0		
B	32.5	354			17.7		
Rb	31.3	426	99	157	137	389	208
Cs	42.5		3.4	5.3	4.7		1.7
Sr	77.4	516	66	3.3	1.4		
Ba	39.3		1300	59			
Pb	37.3	426	17	29	25	54	
Co	34.8	390			0.7		0.2
Ni	38.3	459	5.4	5.5	3		
Cu	37.1	444	2.9	1.4	5		
Zn	42 ?	433	27.1	57	200	327	472
Cr	35		5.5	4.5			
Sc	47 ?			1.5	0.2		0.33
La	36.1	514	25	45	79		246
Ce	38.9	524	48	92	179	275	483
Pr	39.1		5.2		20		
Nd	36.2	505	19	34	81		195
Sm	38.0		3.5	6.9	18		44
Eu	35.6		0.60	0.19	1.4		3.7
Gd	37.7		3.2		19		40
Tb	38.3		0.52	1.3	3.1		8.1
Dy	36.6		3.5		20		
Ho	38.5		0.77		4.2		
Y	37.1	411	27	46	126	237	300
Er	38.4		2.4		13		
Tm	38.1		0.37		1.8		3.8
Yb	40.1		2.7	4.6	13		25
Lu	37.6		0.44	0.69	1.9		3.5
Hf	38.3		3.7	7.2	24		34
Zr	40.3		100	173	1174	1535	1608
Th	38.2	457	9.1	17	17		33
V	38.1						
Nb	38.2		8.7	60	91	315	372
Ta	40.0		0.72	4.0	5.1		21
U	37.2	462	3.5	5.4	4.4		7.3

Concentration of major elements in wt.%, that of trace elements in ppm. Sources of data: NIST-612/613 analyzed for major elements by atomic absorption (Jackson et al. 1992) and for trace elements by solution ICP-MS (Université de Montréal, unpublished data, Jackson et al. 1992, Fedorowich et al. 1993), additional data from NIST data sheets, lithium (L.-H. Chan, unpublished data), beryllium (Domanik et al. 1993), and boron (Gladney & Roelandts 1987); NIST 610/611 analyzed for major elements by electron microprobe at McGill University, trace elements compiled from NIST data sheets, for lithium (L.-H. Chan, unpublished data), beryllium (Domanik et al. 1993), boron (Gladney & Roelandts 1987), and La, Ce, Nd, Y (Hinton 1990); UDM-1 analyzed for major elements by electron microprobe at McGill University and for trace elements by XRF at the Université de Montréal and by solution ICP-MS at Memorial University; DM-0 analyzed by XRF and INAA (Spell 1987); UTR-2 analyzed for major elements by XRF at the University of Toronto and McGill University and for trace elements by XRF and INAA at the University of Toronto and Université de Montréal and by solution ICP-MS at Memorial University; KN-9 analyzed by R. Macdonald by XRF (Macdonald et al. 1987); KE-12 analyzed by R. Macdonald for major elements by XRF at the University of Reading and for trace elements by XRF at the University of Reading and by INAA at the U.S. Geological Survey. Full data compilations for NIST-612, UDM-1, and UTR-2 are found in Appendix 1. * Total iron expressed as Fe_2O_3.

Figures 2a–c show calibration curves for B, Ce, and Y using ^{29}Si and ^{57}Fe as internal standards. Si is the preferred internal standard for felsic glasses because of its much larger abundance compared to Fe. This is particularly so for the NIST standards, which contain only trace levels of Fe, resulting in imprecise analysis by the ICP–MS. The Si-normalized calibration curve for boron passes through the origin and is linear over a range of 33 ppm (Fig. 2a). Other trace elements in felsic rocks can have much larger ranges, with some peralkaline rocks being highly enriched in elements such as the *REE*, Zr, Y, and Nb, among others. This can be seen for the Ce calibration (Fig. 2b), for which the peralkaline rocks contain 179–483 ppm (Table 4). For this calibration, the range of concentrations is approximately 440 ppm Ce. Using both Si and Fe as internal standards, a good linear fit passing through the origin is shown by all standards except KE–12, which is the most Ce-enriched glass. The normalized intensities for KE–12 (which has lower concentrations of Si and Al, and higher concentrations of Na and Fe than do UTR–2 and KN–9, the other peralkaline glasses) plot significantly above this line. Similar behavior is shown for the Y calibration (Fig. 2c), where a range of 260 ppm Y is observed.

Since the Ce and Y intensities for KE–12 both plot above the linear trend on the Si- and Fe-normalized calibrations, we constructed a calibration curve for Y using Ce as the internal standard instead of Si or Fe (Fig. 2d). By doing this, the anomalously high intensity for KE–12 disappears, with all standards now forming a linear trend. These data suggest that for certain trace elements at high concentrations, fractionation can occur between lower-mass major elements and higher-mass trace elements. This is essentially the same behavior as we observed for Zr in the mafic and ultramafic glasses (Fig. 1). As a result, the linear response for the felsic glasses breaks down at high contents of trace elements when using major elements as internal standards. Standard KE–12 contains significantly more iron (9.3 wt.% Fe_2O_3) than the other glasses, and it is possible that this high Fe content suppresses the Si and Fe signals relative to those of Ce and Y. Thus, we appear to be observing a matrix effect. It is important to realize, however, that this matrix effect is observed only at very high concentrations of the trace elements. For the great majority of felsic glasses, which have

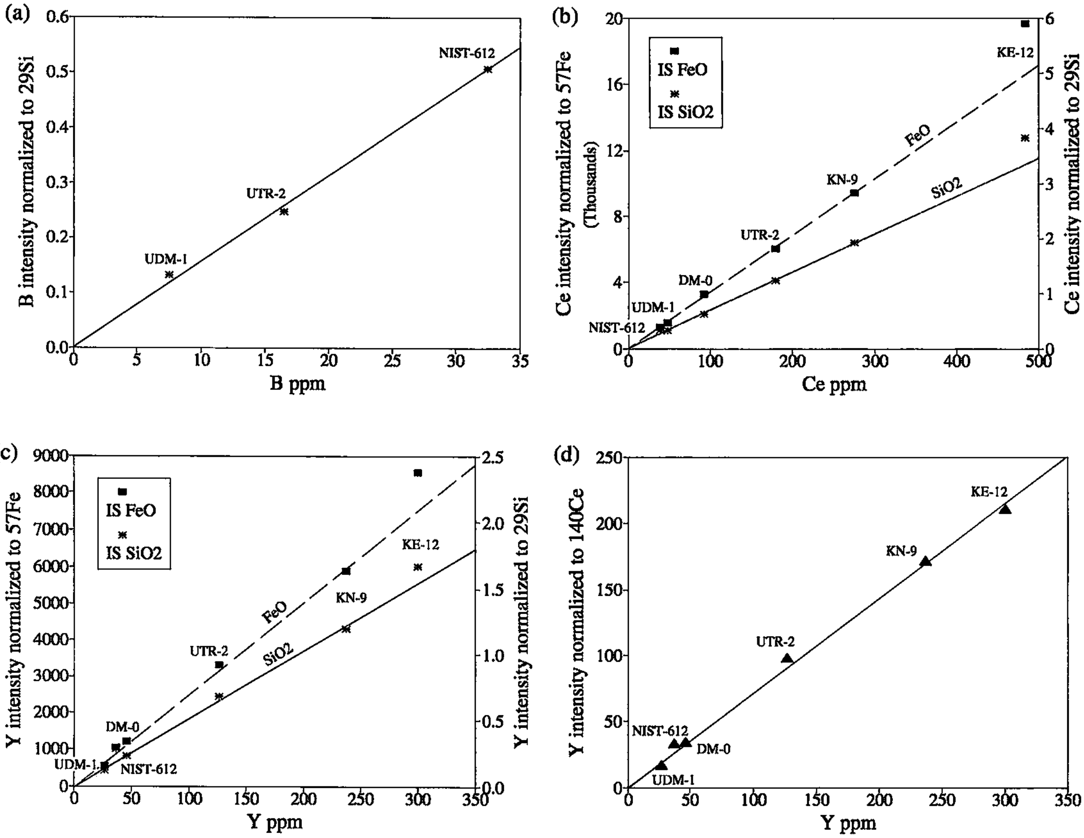

FIG. 2. Calibration of felsic glasses: (a) ^{11}B calibration using ^{29}Si as internal standard (b) ^{140}Ce calibration using ^{29}Si and ^{57}Fe as internal standards, (c) ^{89}Y calibration using ^{29}Si and ^{57}Fe as internal standards, and (d) ^{89}Y calibration using ^{140}Ce as internal standard.

lower concentrations, nonlinearity should not be a problem, and major elements such as Si and Fe can be safely used as internal standards.

Simultaneous calibration of ultramafic, mafic, and felsic glasses

It is difficult to properly calibrate mafic and felsic glasses together because of a lack of suitable internal standards and the generally large differences in concentration of most trace elements between the two types of glasses. For example, Ca and Fe are adequate internal standards for mafic glasses; in felsic glasses, however, their concentrations are too low for practical use. The only internal standard that can be used for both types of glasses is Si. Similarly, Rb concentrations in mafic glasses rarely exceed 50 ppm, whereas felsic glasses can have Rb contents far in excess of this amount. Thus, comparisons can be difficult. Sr is an exception to this rule. It offers the added advantage of being precisely and accurately determined for isotopic work. Figure 3 shows a plot of a Si-normalized Sr calibration for mafic and felsic glasses. The fit is generally good, suggesting that (1) mafic and felsic glasses can be judiciously calibrated together, and (2) matrix effects are less important in the case of Sr.

THE PROBLEM OF ZIRCONIUM, YTTRIUM AND OTHER HIGH-CONCENTRATION TRACE ELEMENTS

The data that we have presented suggest that calibration of Y, Zr, and Ce (and potentially other trace elements) can be difficult under certain conditions. For these elements, the intensity appears to change with respect to that of a major-element internal standard as a function of concentration. This nonlinearity occurs for different internal standards (Si, Ca, Fe) (Figs. 1, 2), so that the problem cannot be attributed to the behavior of one particular internal standard. Nor is it likely a problem of interference. For example, there are no

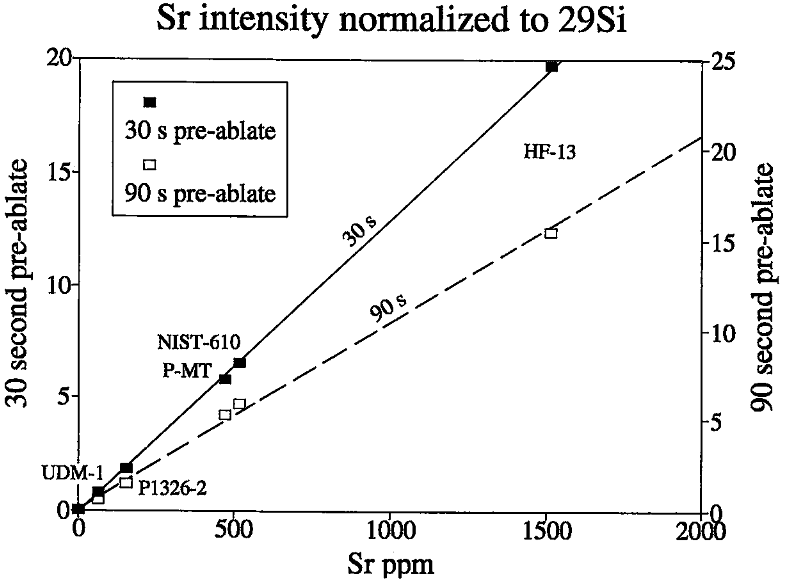

FIG. 3. Calibration curve of ^{88}Sr normalized to ^{29}Si for ultramafic, mafic, and felsic glasses using pre-ablation times of 30 and 90 seconds.

isobaric interferences at masses 89 and 90, and other types of interference (such as polyatomic or oxide species) are not known at these masses (Jarvis *et al.* 1992, Garbe-Schönberg 1993). In fact, the dry ICP–MS plasma, which is used for laser ablation, is remarkably free of interferences. We have compared measured ratios of isotopic abundances for a series of elements (including Zr) for UDM–1, UTR–2, NIST–610, and KE–12 (Fig. 4). For these samples, which have very different contents of trace elements, the observed abundance-ratios are generally similar to natural abundances. The only systematic differences seen are for Li, for which the measured abundance-ratios are slightly low compared to the natural abundance-ratios, and for Pb, for which the measured abundance-ratios are slightly high. The measured and natural abundance ratios for Zr are very similar, which indicates that compositional differences among the samples (*e.g.*, involving iron) do not cause interferences for the two isotopes of Zr, unless each isotope is affected equally by the interference. The general lack of interferences for laser-ablation ICP–MS is a major advantage in comparison to techniques such as secondary-ion mass spectrometry (SIMS), in which polyatomic and oxide interferences can be severe (Shimizu & Hart 1982, Shimizu *et al.* 1978).

Instead, the problem may lie elsewhere, being caused by either large ranges in concentration for these elements, or matrix effects for major or trace elements among different samples, or both. Compared to certain other trace elements (*e.g.*, Sm, Eu), Y, Zr, and Ce show large ranges in concentration in igneous rocks. For example, Ce in our felsic standards has a range in concentration of about 440 ppm, whereas that for Y is 260 ppm. Above a certain range in concentration, the linear nature of the calibration curves for these and other similar elements may break down. It is thus important to try to match standards with unknowns, not only in terms of major-element proportions, but also in terms of trace element contents. In contrast, we note that Sr, which also can have a wide range in concentration in glasses, generally remains linear from 0 to 1500 ppm (Fig. 3).

In the case of basalt standards, it is difficult to explain the nonlinearity of the Zr calibration (Figs. 1b, c) by differences in bulk composition. Whereas the major elements do vary among the samples (Table 3), there are no systematic differences to explain the anomalously high intensities of Zr for HF–13. In contrast, certain major-element concentrations of the rhyolite obsidians do vary systematically with Ce and Y concentrations. As concentration of Ce and Y increases, the Fe and Na contents also increase, and the contents of Al and Si decline. The change in Fe_2O_3 is particularly large, increasing from 0.91 wt.% in UDM–1 to 9.29 wt.% in KE–12. The increases in Ce and Y concentrations also reflect progressive increases in the total trace-element contents of the obsidians (Table 4). It is possible that these differences in bulk composition may play an important role in determining the linearity or nonlinearity of calibration curves for Ce, Y, and other trace elements. For example, different

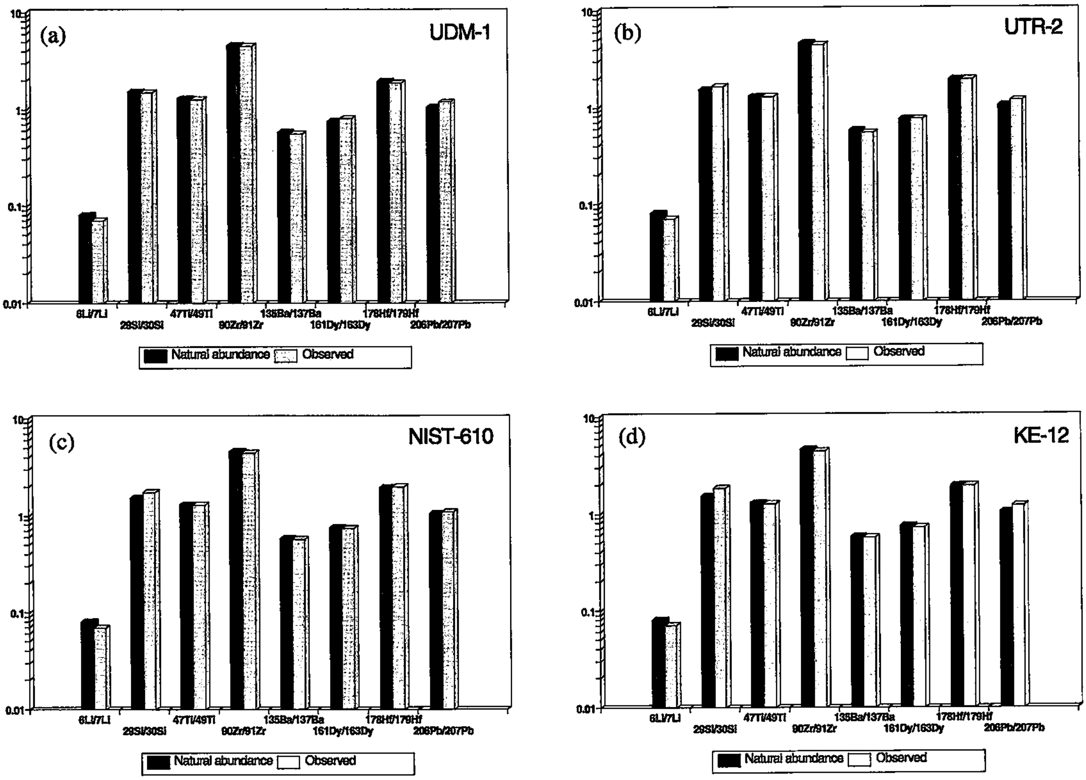

FIG. 4. Measured isotopic abundances for selected major and trace elements in four felsic glass standards using laser ablation ICP–MS. Natural abundances of isotopes are shown for comparison.

contents of iron or trace element among samples may cause differences in laser in absorption and in laser temperature at the sample surface as the laser interacts with the material. Hager (1989) has calculated the effect of temperature on an element's transformation from solid to vapor by the laser beam:

$$n_v \approx n_s \exp(-LM/N_0kT)$$

where n_v is the number of atoms of the element in the vapor, n_s is the number of atoms of the element in the solid, L is the energy required to volatilize the element per unit mass, M is the atomic weight of the element, N_0 is Avogadro's number, k is Boltzmann's constant, and T is the temperature of the solid upon heating by the laser beam. For a Q-switched laser, where sample temperatures are high compared to free-running mode, the energy of volatilization may be better approximated by the ionization potential of the element (Hager 1989).

This equation shows that by raising the temperature in the solid, the efficiency of vaporization will be enhanced. Thus a greater number of atoms will be transported to the ICP–MS in the vapor produced by the laser. More importantly for fractionation between a trace element (*e.g.*, Ce) and its internal standard (*e.g.*, Si), an increase in sample temperature may result in a larger increase of atoms in the vapor for an element with high *LM* (Ce) compared to an element with low *LM* (Si). If there are significant differences in temperature among samples, therefore, fractionation between Ce and Si can occur. The equation also indicates that this fractionation effect is enhanced at lower absolute temperatures. These data suggest that laser-induced sample temperatures for standards HF–13 and KE–12, which plot above the Si-normalized calibration curves for Zr, Ce, and Y, are higher than those for the other glass standards. This results in more Zr, Ce, and Y atoms being volatilized compared to Si, and the Si-normalized intensities for these trace elements being increased. We note that KE–12 is very much darker than the other felsic glasses, and we speculate that it can absorb more laser energy, resulting in higher temperatures.

Single-Standard Calibration

Calibration using a single standard can be advantageous because it saves time during analysis. However, using a single standard for the calibration of unknown samples requires prior establishment of a calibration curve involving this standard and others; this curve must be linear and must pass through the origin. The standard and unknowns also should have similar compositions in terms of major elements. If these conditions are met, single-standard analysis is possible. If these conditions are not met, single-standard calibration will be inaccurate. As an example, Table 5 shows trace-element contents in basalt standard P1326–2 obtained using NIST–612 for calibration. The results using ^{29}Si as the internal standard are clearly too low, whereas the results using ^{44}Ca are generally in agreement with the accepted values. These data indicate that the slopes of the ^{29}Si calibration curves for P1326–2 are lower than those for NIST–612, whereas the slopes of the ^{44}Ca calibration curves for P1326–2 and NIST–612 are about the same. These results can be explained by differences in matrix; SiO_2 in P1326–2 is about 20 wt.% lower than in NIST–612, whereas the CaO contents are nearly identical (Tables 3, 4). Nevertheless, the ^{44}Ca-normalized results for Y and Zr in P1326–2 also are too low because the calibration curves are nonlinear, for reasons discussed above. In this case, NIST–612 is an inappropriate standard with which to calibrate a basalt, particularly for Y and Zr, because they are not matrix-matched. This example highlights the potential pitfalls of using standards that are not similar to unknown samples.

TABLE 5. RESULTS OF LASER-ABLATION ICP-MS ANALYSIS OF JUAN DE FUCA BASALT GLASS P1326-2 USING NIST-612 GLASS AS EXTERNAL CALIBRATION

Element	IS ^{29}Si	IS ^{44}Ca	Accepted
Co ppm	41.1	50.3	47
Ni	40.8	44.0	46
Rb	1.5	1.8	2.2
Sr	121	148	153
Y	20.0	23.0	33
Zr	68.6	80.2	94
Nb	4.7	5.9	4.4
Ba	22.5	27.8	38
La	3.9	4.3	4.7
Ce	10.0	11.8	12.7
Nd	8.0	9.6	10.8
Sm	2.7	3.5	3.4
Eu	1.1	1.4	1.3
Yb	2.2	2.7	3.1
Lu	0.33	0.45	0.44

Sources of accepted values for standard P1326-2 are given in Table 3. IS: internal standard.

Concluding Remarks

In this paper, we demonstrate the importance of using reference standards of similar composition to the unknown samples in calibration of glasses for trace-element analysis by ICP–MS. For certain elements, it appears that matrix effects are minor, and linear calibrations are obtained over a wide compositional spectrum. For other elements, anomalously high intensities were measured in trace-element-rich glass standards. The high intensities may be caused by differences in laser-induced temperatures in the various glasses. Notable differences were obtained between single-standard and multi-standard calibration for Zr and Y. Most users of laser-ablation ICP–MS instruments have calibrated using synthetic glasses that bear little resemblance to natural glasses. However, it is preferable to calibrate using a natural glass whose composition is close to the unknown samples to be analyzed. Glasses can be prepared from pulverized natural rocks and minerals, and we suggest that this is the best approach for analysis of minerals and glasses by laser-ablation ICP–MS.

Acknowledgements

Amira Khoury provided much assistance on the ICP–MS, and Jean-Pierre Bourque meticulously prepared grain mounts for the laser. We thank Claude Dalpé, Don Baker, Brian Cousens, Ray Macdonald, and D.K. Bailey who graciously furnished various glasses and results of geochemical analyses. This work could not have been completed without their help and contributions. The comments of two anonymous reviewers greatly improved the manuscript, and we thank them for their efforts. We also thank Robert F. Martin and Frank C. Hawthorne for their very useful suggestions. This research was supported by NSERC Operating, Infrastructure, Major Installation, and FCAR Equipe grants to JS and JL.

References

Allan, J.F., Chase, R.L., Cousens, B., Michael, P.J., Gorton, M.P. & Scott, S.D. (1993): The Tuzo Wilson volcanic field, NE Pacific: alkaline volcanism at a complex, diffuse, transform-trench-ridge triple junction. *J. Geophys. Res.* **98**, 22367-22387.

Cousens, B.L., Chase, R.L. & Schilling, J.-G. (1985): Geochemistry and origin of volcanic rocks from Tuzo Wilson and Bowie seamounts, northeast Pacific Ocean. *Can. J. Earth. Sci.* **22**, 1609-1617.

Dalpé, C., Baker, D.R. & Sutton, S.R. (1995): Synchrotron X-ray fluorescence and laser ablation ICP–MS microprobes: useful instruments for analysis of experimental run products and other small samples. *Can Mineral.* **33**, 481-498.

DOMANIK, K.J., HERVIG, R.L. & PEACOCK, S.M. (1993): Beryllium and boron in subduction zone minerals: an ion microprobe study. *Geochim. Cosmochim. Acta* **57**, 4997-5010.

FEDOROWICH, J.S., RICHARDS, J.P., JAIN, J.C., KERRICH, R. & FAN, J. (1993): A rapid method for REE and trace-element analysis using laser sampling ICP–MS on direct fusion whole-rock glasses. *Chem. Geol.* **106**, 229-249.

GARBE-SCHÖNBERG, C.-D. (1993): Simultaneous determination of thirty-seven trace elements in twenty-eight international rock standards by ICP–MS. *Geostand. Newslett.* **17**, 81-97.

GLADNEY, E.S. & ROELANDTS, I. (1987): Compilation of boron concentration data for NBS, USGS and CCRMP reference materials. *Geostand. Newslett.* **11**, 167-185.

HAGER, J.W. (1989): Relative elemental responses for laser ablation-inductively coupled plasma mass spectrometry. *Anal. Chem.* **61**, 1243-1248.

HINTON, R.W. (1990): Ion microprobe trace-element analysis of silicates: measurement of multi-element glasses. *Chem. Geol.* **83**, 11-25.

JACKSON, S.E., LONGERICH, H.P., DUNNING, G.R. & FRYER, B.J. (1992): The application of laser ablation microprobe-inductively coupled plasma-mass spectrometry (LAM–ICP–MS) to in-situ trace element determinations in minerals. *Can. Mineral.* **30**, 1049-1064.

JARVIS, K.E., GRAY, A.L. & HOUK, R.S. (1992): *Handbook of Inductively Coupled Plasma Mass Spectrometry*. Blackie, Glasgow, U.K.

________ & WILLIAMS, J.G. (1993): Laser ablation inductively coupled plasma mass spectrometry (LA–ICP–MS): a rapid technique for the direct, quantitative determination of major, trace and rare-earth elements in geological samples. *Chem. Geol.* **106**, 251-262.

JENNER, G.A., FOLEY, S.F., JACKSON, S.E., GREEN, T.H., FRYER, B.J. & LONGERICH, H.P. (1993): Determination of partition coefficients for trace elements in high pressure – temperature experimental run products by laser ablation microprobe – inductively coupled plasma – mass spectrometry (LAM–ICP–MS). *Geochim. Cosmochim. Acta* **57**, 5099-5103.

MACDONALD, R., DAVIES, G.R., BLISS, C.M., LEAT, P.T., BAILEY, D.K. & SMITH, R.L. (1987): Geochemistry of high-silica peralkaline rhyolites, Naivasha, Kenya Rift Valley. *J. Petrol.* **28**, 979-1008.

PEARCE, N.J.G., PERKINS, W.T., ABELL, I., DULLER, G.A.T. & FUGE, R. (1992): Mineral microanalysis by laser ablation inductively coupled plasma mass spectrometry. *J. Anal. Atom. Spectrom.* **7**, 53-57.

PERKINS, W.T., PEARCE, N.J.G. & FUGE, R. (1992): Analysis of zircon by laser ablation and solution inductively coupled plasma mass spectrometry. *J. Anal. Atom. Spectrom.* **7**, 611-616.

PERKINS, W.T., PEARCE, N.J.G. & JEFFRIES, T.E. (1993): Laser ablation inductively coupled plasma mass spectrometry: a new technique for the determination of trace and ultratrace elements in silicates. *Geochim. Cosmochim. Acta* **57**, 475-482.

SHIMIZU, N. & HART, S.R. (1982): Applications of the ion microprobe to geochemistry and cosmochemistry. *Annu. Rev. Earth Planet. Sci.* **10**, 483-526.

________, SEMET, M.P. & ALLÈGRE, C.J. (1978): Geochemical applications of quantitative ion-microprobe analysis. *Geochim. Cosmochim. Acta* **42**, 1321-1334.

SPELL, T.L. (1987): *Geochemistry of Valle Grande Member Ring Fracture Rhyolites, Valles Caldera, New Mexico.* M.S. thesis, New Mexico Institute of Mining and Technology, Socorro, New Mexico.

Received March 29, 1994, revised manuscript accepted February 2, 1995.